

**A synthetic strategy for the preparation of sub-100 nm  
functional polymer particles of uniform diameter**

Journal:	<i>Polymer Chemistry</i>
Manuscript ID:	PY-COM-12-2014-001703.R1
Article Type:	Communication
Date Submitted by the Author:	19-Dec-2014
Complete List of Authors:	Killops, Kato; Edgewood Chemical Biological Center, Rodriguez, Christina; Lawrence Berkeley National Laboratory, Joint Center for Artificial Photosynthesis Lundberg, Pontus; Thermo Fisher Scientific, Life Sciences Solutions Hawker, Craig; University of California, Materials Research Laboratory Lynd, Nathaniel; Lawrence Berkeley National Laboratory, Joint Center for Artificial Photosynthesis

## COMMUNICATION

## A synthetic strategy for the preparation of sub-100 nm functional polymer particles of uniform diameter

Cite this: DOI: 10.1039/x0xx00000x

Kato L. Killops,<sup>a\*</sup> Christina G. Rodriguez,<sup>b,c</sup> Pontus Lundberg,<sup>d</sup> Craig J. Hawker,<sup>c</sup> and Nathaniel A. Lynd<sup>b,c,e\*</sup>

Received 00th January 2012,  
Accepted 00th January 2012

DOI: 10.1039/x0xx00000x

www.rsc.org/

**An amphiphilic block copolymer surfactant is used to impart peripheral surface functionality to polymer nanoparticles synthesized via emulsion polymerization. Particles ranged in size from ca. 55 nm by SEM (ca. 82 nm by DLS) to just over 200 nm. Particles displaying latent functionality were readily functionalized directly after polymerization using a fluorescent dye.**

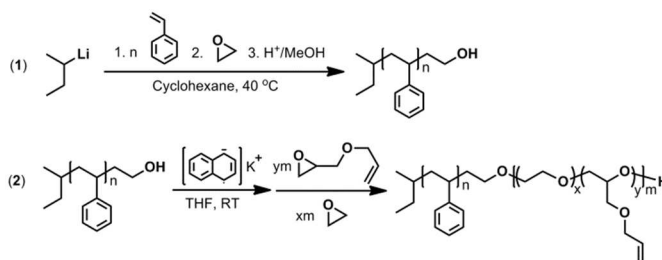
Functional polymer nanoparticles form the basis of important emerging technology platforms used in the life sciences. For example, functional mesoscopic (<1µm) spheres are integral to ion semiconductor-based rapid DNA sequencing<sup>1</sup> and *in vitro* diagnosis exploiting antibody-antigen interactions.<sup>2</sup> In ion semiconductor DNA sequencing, functional, uniform diameter polymer spheres are conjugated on their periphery with sample DNA templates that, when used to polymerize a complementary strand, release protons registering a change in potential when the complementary sequence is polymerized.<sup>3</sup> Speed, accuracy, and the number of base pairs that can be sequenced per semiconductor chip improve by further miniaturizing chip features. This miniaturization, however, requires a reduction in sphere size. Further improvements in ion semiconductor DNA sequencing thus benefit directly from decreasing polymer sphere size while retaining narrow size dispersity and high surface functionality. Decreasing sphere size is directly correlated with the cost to sequence a human genome.

In order to synthesize colloidal polymer particles at the nanoscale size regime with tunable peripheral functionality, emulsion or dispersion polymerization techniques may be employed.<sup>4</sup> Emulsion polymerization techniques are highly amenable to industrial processes due to ease of scalability and the use of water as the solvent. While our primary interest is biomedical, the possibility to tailor the particle functionality lies at the nexus of advanced purification strategies,<sup>5, 6</sup> as well as expanding

opportunities for photonic materials,<sup>7</sup> smart coatings,<sup>8, 9</sup> and abiotic-biological interfaces.<sup>10, 11</sup>

Many strategies exist for achieving functional polymer colloids.<sup>12, 13</sup> Mixing a range of monomers in desired proportions can lead to particles with diverse functionality *via* emulsion polymerization.<sup>14, 15</sup> Other common approaches include incorporation of reactive surfactants or surfimers<sup>16</sup> (surfactant monomers) to achieve peripheral functionality. An alternative approach is to use amphiphilic block copolymers (BCPs) as surfactants to stabilize emulsion particles, resulting in latexes with a polymer corona.<sup>17-19</sup> Although a number of different BCPs have been used, polystyrene-*b*-poly(ethylene oxide) (PS-*b*-PEO) has been widely studied in emulsion polymerizations.<sup>20-22</sup> However, PS-*b*-PEO lacks the capacity to be further modified or functionalized.

**Scheme 1.** Anionic synthesis of (1) PS macroinitiator followed by (2) addition of P(EO-*co*-AGE) block.



The use of BCP stabilizers confers a number of advantages over their small molecule counterparts including low critical micelle concentrations and low diffusion coefficients, which aid in anchoring the macromolecules to the particle interface.<sup>23</sup> Our approach capitalizes on the opportunity for macromolecules to provide multiple modular functional groups on a single stabilizer molecule. Furthermore, the advantage of using a functional BCP

Table 1. Block copolymer functional surfactant precursors.

Polymer Group	Name	$M_n$ PS <sup>a</sup> [g/mol]	DP PEO <sup>b</sup>	DP PAGE <sup>b</sup>	Mol % AGE <sup>c</sup>	Total $M_n$ <sup>b</sup> [g/mol]	PDI <sup>a</sup>	HLB
PS <sub>5k</sub> -b-P(EO-co-AGE <sub>3%</sub> ) <sub>15k</sub>	<b>S3</b>	5,000	320	8	3	20,000	1.08	14
PS <sub>11k</sub> -b-P(EO-co-AGE <sub>1%</sub> ) <sub>50k</sub>	<b>M1</b>	11000	1110	10	1	61,200	1.05	16
PS <sub>11k</sub> -b-P(EO-co-AGE <sub>3%</sub> ) <sub>50k</sub>	<b>M3</b>	11000	960	28	3	56,600	1.04	15
PS <sub>11k</sub> -b-P(EO-co-AGE <sub>5%</sub> ) <sub>50k</sub>	<b>M5</b>	11000	1000	58	5	61,800	1.06	14
PS <sub>16k</sub> -b-P(EO-co-AGE <sub>3%</sub> ) <sub>90k</sub>	<b>L3</b>	16000	1860	53	3	104,000	1.09	16

<sup>a</sup> Determined by SEC relative to PS standards. <sup>b</sup> Degree of polymerization (DP) determined by <sup>1</sup>H NMR. <sup>c</sup> From monomer feed.

platform is that a single precursor polymer can be modified with a variety of functional groups in order to create a library of functional particles.

Herein, we demonstrate the synthesis of PS-based latexes with tunable peripheral functionality by starting from a PS-*b*-poly[(ethylene oxide)-*co*-(allyl glycidyl ether)] [PS-*b*-P(EO-*co*-AGE)] amphiphilic BCP (Figure 1).<sup>24, 25</sup> The incorporation of an allyl-functional monomer (AGE) into the hydrophilic portion of the BCP enables the use of thiol-ene “click” chemistry<sup>26</sup> to decorate the polymer backbone with a diverse range of thiol functional groups. In this report, we examine synthetic strategies for sub-100nm uniform particles and carry out functionalization of the particle surface.

An amphiphilic BCP scaffold, PS-*b*-P(EO-*co*-AGE), was devised to serve as an emulsion polymerization stabilizer to synthesize sub-100 nm PS particles with uniform size and peripheral functionality. The PS block is identical in composition to the bulk of the resultant polymer particle, serving to anchor the BCP to the particle. The hydrophilic P(EO-*co*-AGE) block extends into the aqueous reaction medium and stabilizes the PS particles. The allyl groups distributed along the P(EO-*co*-AGE) backbone permit pre- or post-polymerization functionalization with a range of thiol-functional moieties. Hydroxy-terminal PS macroinitiators were synthesized in large batches *via* standard anionic polymerization,<sup>27</sup> followed by copolymerization of EO and AGE to give PS-*b*-P(EO-*co*-AGE) BCPs in large (>10g) quantities. A range of PS-*b*-P(EO-*co*-AGE) BCPs were synthesized for an initial screen of the effects of molecular weight and AGE incorporation on particle formation. Small (S), medium (M), and large (L) BCPs were synthesized based on 5, 11, and 16 kg/mol PS blocks, respectively (Table 1). Because the relative weight percentages of the hydrophilic and hydrophobic blocks are of critical importance to water-solubility, micellization, and emulsion stabilization,<sup>28</sup> hydrophilic block weight percentages for all polymers synthesized were in the range of 75 to 85 wt.%. The BCPs were characterized by size exclusion chromatography (SEC) and <sup>1</sup>H NMR spectroscopy (Figures S1 and S2 for **M3**, representative). Incorporation of the functional AGE monomer ranged from 1 to 5 mol.% relative to EO repeat units. Furthermore, the calculated hydrophilic-lipophilic balance (HLB) for each polymer resides in the range of 14–16, where values greater than 12 are predicted to stabilize oil-in-water emulsions.<sup>29</sup>

The amphiphilic BCPs formed aggregated structures in aqueous solution, and dynamic light scattering (DLS) was carried out to investigate the size of the structures. Solutions with concentrations of 0.1 mg/mL were measured, well above the critical micelle concentration (CMC) for PS-*b*-PEO systems.<sup>30</sup> All BCPs except **L3** exhibited a monomodal population with broad size polydispersity (Figure S3a). Without performing solvent exchange

and dialysis on the BCP solutions, a micellar aggregate population is primarily observed.<sup>31, 32</sup> The hydrodynamic diameter ( $D_h$ ) of the aggregates increases with BCP molecular weight from 156 nm for **S3** to 389 nm for **L3** (Table S1). After the addition of styrene, the swollen structures exhibit  $D_h$  values that range from 130 nm to 182 nm (Figure S3b, Table S2), and no longer correlate with BCP molecular weight.

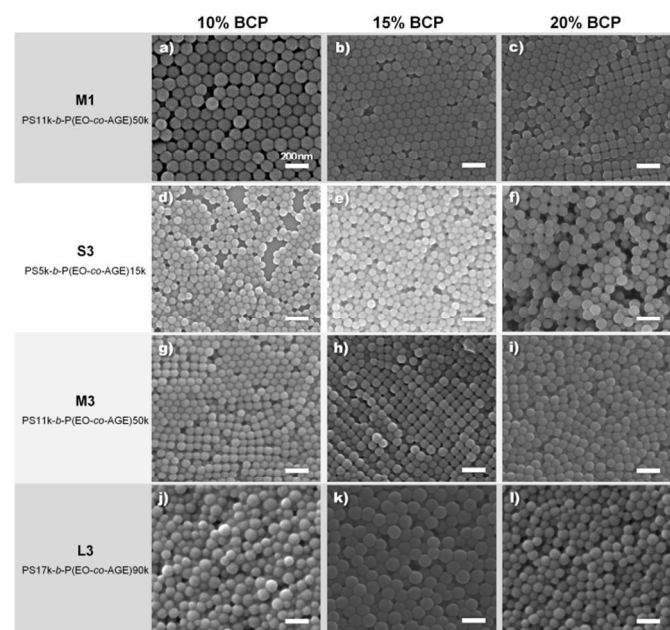


**Figure 1.** SEM images of particles synthesized with different BCP stabilizers and varying incorporations of BCP stabilizer. All scale bars are 200nm.

Emulsion polymerizations were carried out in large batches containing water, styrene, potassium persulfate, and PS-*b*-P(EO-*co*-AGE) as the only emulsion stabilizer. Initially, alkene functional particles were prepared using BCP **M1**. Particle size was determined by SEM and DLS (Table 2, Figure S4). Most of the particle diameters measured by DLS were larger than those measured by SEM. Measurements by DLS provide  $D_h$  of the particles, including the solvated corona, whereas in SEM that layer is collapsed. In the case of **S3** 20%, **M3** 5%, and **L3** 10%, the sizes measured by the two techniques fall within the polydispersity range. Furthermore, the overall concentration of BCP in **M3** 5% and **L3** 10% is quite low (80 and 87 $\mu$ M, respectively), leading to sparsely populated corona and smaller apparent  $D_h$ . Coefficients of variation (CV) were calculated from SEM diameters and were found to exist

in the region  $\leq 5\%$  for most samples. Conventionally, a system with a CV  $\leq 10\%$  is considered monodisperse.<sup>33</sup> The amount of BCP stabilizer had a substantial effect on the final diameter of the particles for polymer **M1**. A marked decrease in diameter was observed upon increasing the **M1** content from 10 wt.% to 15 wt.%, and less dramatically upon increasing the BCP content further, from 15 to 20 wt.%. Similarly, particles synthesized using 5 wt.% **M3** were larger and more polydisperse, but decreased in size and polydispersity upon increasing BCP incorporation to 10 wt.% and above. Others have found that both reaction rate and final particle size were closely correlated to the concentration of PS-*b*-PEO in emulsion polymerization.<sup>20, 22, 34</sup> In order to determine the effect of molecular weight on particle formation in this system, our BCP library was expanded to include BCPs consisting of smaller (**S3**) and larger (**L3**) molecular weights relative to **M3**, while keeping the weight percentage of PS near 20%.

Figure 1 shows representative SEM images of particles

**Table 2.** Average diameters of polymer particles with varying BCP incorporation.

BCP Used	Wt. % BCP	[BCP] ( $\times 10^{-4}$ M)	$D_h^a$ (nm)	% PD <sup>a</sup>	$D_{SEM}^b$ (nm)	CV <sub>SEM</sub> <sup>b</sup> (%)
None	0	0	299	20	280 ± 13	4.6
<b>S3</b>	10	4.6	92	34	55 ± 2	3.6
<b>S3</b>	15	6.8	104	22	62 ± 3	4.8
<b>S3</b>	20	9.1	83	20	86 ± 4	4.7
<b>M1</b>	10	1.5	196	48	100 ± 4	4.0
<b>M1</b>	15	2.2	162	52	80 ± 2	2.5
<b>M1</b>	20	3.0	150	28	77 ± 1	1.3
<b>M3</b>	5	0.8	174	14	185 ± 71	38.4
<b>M3</b>	10	1.6	104	14	72 ± 3	4.2
<b>M3</b>	15	2.4	106	11	75 ± 4	5.3
<b>M3</b>	20	3.2	124	10	74 ± 4	5.4
<b>M5</b>	10	1.5	c	–	c	–
<b>L3</b>	10	0.9	136	28	141 ± 7	5.0
<b>L3</b>	15	1.3	150	14	110 ± 3	2.7
<b>L3</b>	20	1.8	137	24	82 ± 13	15.9

<sup>a</sup>  $D_h$  and % polydispersity (PD) determined by DLS using Wyatt Dynamics software. <sup>b</sup> Determined by SEM using ImageJ software. <sup>c</sup> Inconclusive due to large size polydispersity.

formed at a range of BCP incorporations and varying molecular weight and AGE incorporation. Particles formed from **M1** had low polydispersity, and SEM showed a decrease in particle size with increasing BCP incorporation.<sup>22</sup> For **M3**, the size decrease visualized by SEM followed the same trend as observed by DLS. These monodisperse particles had a propensity to crystallize into iridescent colloidal arrays. This trend was not repeated in the case of the series of particles derived from **S3** and **L3** where particle diameter did not correlate with BCP incorporation. For **S3**, the size of the particles measured by SEM increased with increasing BCP content. This was likely due to the availability of more chains such that larger monomer droplets could be stabilized against coalescence without the steric effects that hinder the packing of larger BCPs into growing particles.<sup>32</sup> In the case of **L3**, the number of chains available for stabilization was lower, leading to decreased stability of growing

droplets and increased polydispersity. Lower diffusion coefficients of large BCPs caused them to become entrapped within the particles more easily, where they were unavailable to stabilize the interface.<sup>20</sup> The number of particles,  $N_p$ , was also found to generally increase with BCP loading (Figure S5).<sup>21, 34</sup> At higher BCP concentrations, more micelles were available for nucleation and a larger number of particles could be stabilized.<sup>23</sup>

We synthesized BCPs with varying levels of AGE in the hydrophilic block to maximize reactive functionality while maintaining control over particle formation. Because syntheses with **M1** and **M3** yielded well-defined particles, we attempted to maximize the AGE incorporation with **M5**, which contained 5 mol.% AGE. Particles synthesized with **M5** coagulated or were quite polydisperse, as compared to the analogous **M1** and **M3** particles with low CV values (Figure S6a and b). The increased concentration of alkene groups on **M5** likely caused additional interparticle coupling that is not observed with lower AGE incorporations.

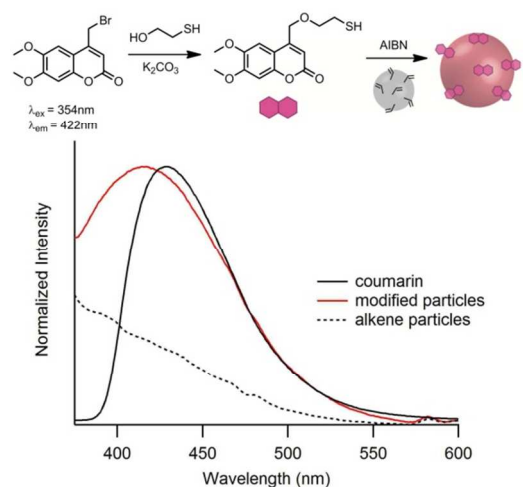


**Figure 2.** Fluorescence spectra of thiol-functional coumarin coupling to the latent surface functionality on **M3** particles (15% BCP) using thermally-initiated thiol-ene click chemistry.

The ability to modify the particle surface after polymerization is critical for advanced biomedical applications. Although some of the allyl groups may react during the course of polymerization, their reactivity and concentration are significantly lower than that of styrene,<sup>35</sup> and most survive the polymerization. To probe the survival of surface active allyl groups after particle synthesis, a thiol-functional coumarin dye was synthesized (see Figure 2, S7 and S8). Thermally-initiated thiol-ene coupling between particles (**M3**, 15 wt.% BCP) and thiol-functional coumarin was carried out using AIBN initiator in methanol. DLS measurements of the particles before reaction and after purification show a slight increase in  $R_h$  as well as polydispersity (Figure S9). We postulate that the increase in hydrophobic character at the particle periphery is partially responsible for the increase in polydispersity and size, as these particles are more likely to aggregate. The fluorescence spectrum of a purified solution of labeled particles shown in Figure 2 was consistent with the surface attachment of coumarin to the polymer particle surface, with an accompanying blue shift in the spectrum,<sup>36</sup> indicating survival of the surface functionality on the 75 nm diameter particles after polymerization. Due to the unreliable nature of surface functionalization quantification using fluorescence

spectroscopy,<sup>37</sup> the extent of functionalization could not be calculated.

## Conclusions

In this report, we describe a new approach for the synthesis of functional polymeric particles with sub-100 nm uniform diameters. Using block copolymer stabilizers for the emulsion polymerization, the resultant polymer particles reached diameters as low as 55 nm as measured by SEM, with a standard deviation of 2 nm. The existence of surface functionality was inferred *via* reaction with a coumarin dye, which exhibited distinct fluorescence when coupled to the functional particles. The development of new concepts in sub-100 nm functional polymer sphere synthesis offers new routes to decrease device size, or increase information density on semiconductor-based *in vitro* technologies that utilize polymer spheres of uniform diameter and defined surface functionality.

## Notes and references

<sup>a</sup> U.S. Army Edgewood Chemical Biological Center, Aberdeen Proving Ground, MD 21010. Email: kathryn.l.killops.civ@mail.mil

<sup>b</sup> Joint Center for Artificial Photosynthesis, Lawrence Berkeley National Laboratory, Berkeley, CA 94720.

<sup>c</sup> Materials Research Laboratory, University of California, Santa Barbara, CA 93106.

<sup>d</sup> Life Sciences Solutions, Thermo Fisher Scientific, Svellevieien 29, 2001, Lillestrøm, Norway.

<sup>e</sup> McKetta Department of Chemical Engineering, University of Texas at Austin, Austin, TX 78712. Email: lynd@che.utexas.edu

† Electronic Supplementary Information (ESI) available: Experimental details, NMR, GPC, DLS, and SEM. See DOI: 10.1039/c000000x/

‡ This research is funded by the Department of the Army Basic Research Program and sponsored by the Edgewood Chemical Biological Center. Funding for C.R. was provided by the Army Research Office through the Institute for Collaborative Biotechnologies at University of California, Santa Barbara under award number W911NF-09-D-0001-0028. This work was partially supported by the MRSEC Program of the National Science Foundation under Award No. DMR 1121053.

- J. M. Rothberg, W. Hinz, T. M. Rearick, J. Schultz, W. Mileski, M. Davey, J. H. Leamon, K. Johnson, M. J. Milgrew, M. Edwards, J. Hoon, J. F. Simons, D. Marran, J. W. Myers, J. F. Davidson, A. Branting, J. R. Nobile, B. P. Puc, D. Light, T. A. Clark, M. Huber, J. T. Branciforte, I. B. Stoner, S. E. Cawley, M. Lyons, Y. Fu, N. Homer, M. Sedova, X. Miao, B. Reed, J. Sabina, E. Feierstein, M. Schorn, M. Alanjary, E. Dimalanta, D. Dressman, R. Kasinskas, T. Sokolsky, J. A. Fianza, E. Namsaraev, K. J. McKernan, A. Williams, G. T. Roth and J. Bustillo, *Nature*, 2011, 475, 348-352.
- M. Mahmoudi, I. Lynch, M. Ejtehadi, M. Monopoli, F. Bombelli and S. Laurent, *Chem. Rev.*, 2011, 111, 5610-5637.
- B. Merriman and J. M. Rothberg, *Electrophoresis*, 2012, 33, 3397-3417.
- Emulsion Polymerization and Emulsion Polymers*, ed. P. A. Lovell and M. S. El-Aasser John Wiley & Sons, New York, 1997.
- B. Wei, B. J. Rogers and M. J. Wirth, *J. Am. Chem. Soc.*, 2012, 134, 10780-10782.
- M. A. Daniele, Y. P. Bandera, D. Sharma, P. Rungta, R. Roeder, M. G. Sehorn and S. H. Foulger, *Small*, 2012, 8, 2083-2090.
- S.-H. Kim, S. Lee, S.-M. Yang and G.-R. Yi, *NPG Asia Materials*, 2011, 3, 25-33.
- A. Muñoz-Bonilla, A. M. Herk and J. P. A. Heuts, *Macromolecules*, 2010, 43, 2721-2731.
- A. Muñoz-Bonilla, A. M. Herk and J. P. A. Heuts, *Polym. Chem.*, 2010, 1, 624.
- R. F. Fakhru'llin and Y. M. Lvov, *ACS Nano*, 2012, 6, 4557-4564.
- S.-H. Lee, Y. Hoshino, A. Randall, Z. Zeng, P. Baldi, R.-a. Doong and K. J. Shea, *J. Am. Chem. Soc.*, 2012, 134, 15765-15772.
- N. Warren and S. Armes, *J. Am. Chem. Soc.*, 2014, 136, 10174-10185.
- B. Charleux, G. Delaître, J. Rieger and F. D'Agosto, *Macromolecules*, 2012, 45, 6753-6765.
- P. Bolt, J. Goodwin and R. Ottewill, *Langmuir*, 2005, 21, 9911-9916.
- J. Ramos, J. Forcada and R. Hidalgo-Alvarez, *Chem. Rev.*, 2014, 114, 367-428.
- S. Pargen, C. Willems, H. Keul, A. Pich and M. Möller, *Macromolecules*, 2012, 45, 1230-1240.
- G. Riess, *Prog. Polym. Sci.*, 2003, 28, 1107-1170.
- L. Li, J. Yang and J. Zhou, *Macromolecules*, 2013, 46, 2808-2817.
- C. Burguière, S. Pascual, C. Bui, J.-P. Vairon, B. Charleux, K. Davis, K. Matyjaszewski and I. Bétremieux, *Macromolecules*, 2001, 34, 4439-4450.
- J.-L. Mura and G. Riess, *Polym. Adv. Technol.*, 1995, 6, 497-508.
- G. Jialanella, E. Firer and I. Piirma, *J. Polym. Sci., Part A: Polym. Chem.*, 1992, 30, 1925-1933.
- M. Berger, W. Richtering and R. Mülhaupt, *Polym. Bull.*, 1994, 33, 521-528.
- G. Riess and C. Labbe, *Macromol. Rapid Commun.*, 2004, 25, 401-435.
- M. D. Dimitriou, Z. Zhou, H.-S. Yoo, K. L. Killops, J. A. Finlay, G. Cone, H. S. Sundaram, N. A. Lynd, K. P. Barteau, L. M. Campos, D. A. Fischer, M. E. Callow, J. A. Callow, C. K. Ober, C. J. Hawker and E. J. Kramer, *Langmuir*, 2011, 27, 13762-13772.
- B. Lee, M. J. Kade, J. A. Chute, N. Gupta, L. M. Campos, G. H. Fredrickson, E. J. Kramer, N. A. Lynd and C. J. Hawker, *J. Polym. Sci., Part A: Polym. Chem.*, 2011, 49, 4498-4504.
- K. L. Killops, L. M. Campos and C. J. Hawker, *J. Am. Chem. Soc.*, 2008, 130, 5062-5064.
- K. L. Killops, N. Gupta, M. D. Dimitriou, N. A. Lynd, H. Jung, H. Tran, J. Bang and L. M. Campos, *ACS Macro Letters*, 2012, 1, 758-763.
- I. Piirma, in *Surfactant Science Series 42*, Marcel Dekker, New York, 1992, ch. 1.
- S. Garnier and A. Laschewsky, *Langmuir*, 2006, 22, 4044-4053.
- M. Wilhelm, C. L. Zhao, Y. Wang, R. Xu, M. A. Winnik, J. L. Mura, G. Riess and M. D. Croucher, *Macromolecules*, 1991, 24, 1033-1040.
- R. Xu, M. A. Winnik, F. R. Hallett, G. Riess and M. D. Croucher, *Macromolecules*, 1991, 24, 87-93.
- C. L. Winzor, Z. Mrázek, M. A. Winnik, M. D. Croucher and G. Riess, *Eur. Polym. J.*, 1994, 30, 121-128.
- J. Goodwin, *Colloids and Interfaces with Surfactants and Polymers: An Introduction*, ed. Wiley, West Sussex, England, 2004.
- G. Riess, *Colloids Surf., A*, 1999, 153, 99-110.

## Journal Name

35. F. Mayo, F. Lewis and C. Walling, *J. Am. Chem. Soc.*, 1948, 70, 1529-1533.
36. G. Jones, W. Jackson, C. Choi and W. Bergmark, *J. Phys. Chem.*, 1985, 89, 294-300.
37. A. Hennig, H. Borchering, C. Jaeger, S. Hatami, C. Würth, A. Hoffmann, K. Hoffmann, T. Thiele, U. Schedler and U. Resch-Genger, *J. Am. Chem. Soc.*, 2012, 134, 8268-8276.